Biochimica et Biophysica Acta 1818 (2012) 1691–1697

Contents lists available at SciVerse ScienceDirect

Biochimica et Biophysica Acta

journal homepage: www.elsevier.com/locate/bbamem

Similar structures but different mechanisms
Prediction of FABPs–membrane interaction by electrostatic calculation

Fernando Zamarreño [a], Fernando E. Herrera [b], Betina Córsico [c], Marcelo D. Costabel [a,*]

[a] Grupo de Biofísica, Departamento de Física, Universidad Nacional del Sur, Bahía Blanca, Argentina
[b] Departamento de Física, Facultad de Bioquímica y Ciencias Biologicas, Universidad Nacional del Litoral, Santa Fe, Argentina
[c] Instituto de Investigaciones Bioquímicas de La Plata (CONICET-UNLP), Facultad de Ciencias Médicas, Universidad Nacional de La Plata, Argentina

ARTICLE INFO

Article history:
Received 22 December 2011
Received in revised form 27 February 2012
Accepted 7 March 2012
Available online 14 March 2012

Keywords:
Fatty acid binding protein
Electrostatic interaction
Protein–membrane interaction
Molecular dynamics simulation
Biomolecular modeling
Structure–function relation

ABSTRACT

The role of fatty acid binding proteins as intracellular fatty acid transporters may require their direct interaction with membranes. In this way different mechanisms have been previously characterized through experimental studies suggesting different models for FABPs–membrane association, although the process in which the molecule adsorbs to the membrane remains to be elucidated. To estimate the importance of the electrostatic energy in the FABP–membrane interaction, we computationally modeled the interaction of different FABPs with both anionic and neutral membranes. Free Electrostatic Energy of Binding (dE), was computed using Finite Difference Poisson Boltzmann Equation (FDPB) method as implemented in APBS (Adaptive Poisson Boltzmann Solver). Based on the computational analysis, it is found that recruitment to membranes is facilitated by non-specific electrostatic interactions. Also energetic analysis can quantitatively differentiate among the mechanisms of membrane association proposed and determinate the most energetically favorable configuration for the membrane-associated states of different FABPs. This type of calculations could provide a starting point for further computational or experimental analysis.

1. Introduction

The study of reversible protein-membrane interactions constitutes a challenge to biophysics, and has a deep impact in biotechnology and medicine. These highly-complex and crucial biological processes can be conceptually separated into several steps, such as primary electrostatic attraction, increase in the effective local concentration and spatial orientation of the protein, desolvation and interfacial water reorganization, protein conformational changes, and restructuring of the lipid bilayer. Moreover, in some cases, binding is followed by insertion into the membrane and subsequent specific interactions with inner membrane components, lipids and proteins.

Several systems, such as binding of cytochrome *c* to anionic lipid membranes [1,2] or binding of antimicrobial, amphipatic peptides to bacteria and red cell membranes [3–5] have been extensively studied. Other cases that attracted considerable interest are interaction of regulatory peptides with membrane channels [6], membrane effects of apoptotic proteins [7,8], viral infection and membrane fusion [9–15], lipid delivery to tissues and cells [16–18], and peptide mediated gene transfer [19].

Protein-membrane interactions that enhance lipid transfer between different organelles are also a prominent subject of study. Examples of this kind are fatty acid binding proteins (FABPs), sterol carrier protein 2 (SCP2) and acyl–CoA binding protein (ACBP), all of which have been implicated in processes that facilitate lipid solubilization and movement in the cellular milieu [20–24], and for which, their interactions with membranes have been experimentally demonstrated [25–27].

Fatty acid-binding proteins (FABPs) are intracellular proteins expressed in almost all animal tissues in different isoforms. It is proposed that they transport and target fatty acids (FA) to specific membranes and metabolic pathways. Several studies have suggested that different FABPs have unique functions and this specificity may be driven, in part, by protein–membrane interactions [28–30].

Structurally, FABPs are proteins of approximately 14 kDa of molecular weight with low amino acid sequence homology but sharing a common tertiary structure consisting of 10 antiparallel β-strands that form a β-barrel, which is capped by two short α-helices arranged as a helix-turn-helix segment [31,32].

It is proposed that FABPs may serve not only to deliver long-chain fatty acids to target organelles, but also to remove surface membrane-bound fatty acids, and this may require their direct interaction with acceptor membranes and ligand donor [22,33]. In vitro studies have shown that different FABPs transfer FA to membranes by two different transfer mechanisms. A larger number of the FABPs, including intestinal (IFABP), brain (BFABP), adipocyte (AFABP) and heart

* Corresponding author at: Grupo de Biofísica, Departamento de Física, Universidad Nacional del Sur, Avda. Alem 1253, (8000) Bahía Blanca, Argentina. Tel.: +54 291 4595101x2805; fax: +54 291 4595142.
E-mail address: costabel@criba.edu.ar (M.D. Costabel).

0005-2736/$ – see front matter © 2012 Elsevier B.V. All rights reserved.
doi:10.1016/j.bbamem.2012.03.003

(HFABP) types, transfer their FAs by directly interacting with membranes ("collisional" FABPs). In marked contrast, other members of the family, as liver FABP (LFABP) and CRBPII, transfer their ligands to and from membranes by an aqueous-diffusion mediated mechanism ("diffusional" FABPs) [22].

Many studies have provided substantial evidence demonstrating IFABP interaction with membranes, and have shown that electrostatic and hydrophobic forces modulate these physical interactions [34,38]. In contrast, LFABP has been classically considered a "diffusional" FABP, based on FA transfer kinetic studies. Recent studies which analyzed I- and LFABP's capacity to directly interact with membranes, employing different experimental approaches, have shown that LFABP is also able to interact with phospholipid membranes [39]. It was also demonstrated that the factors that modulate this process are different for each protein, implying different roles for IFABP and LFABP in an intracellular context.

In this work, FABPs belonging to several sources have been considered for this computational analysis. The selected proteins belong to either the "collisional" or "difussional" group. Computational methods have been immensely useful in the analysis of stability, dynamics, and association of proteins, nucleic acids, and other biological molecules [40–42]. They can provide models with atomic detail for interactions involving a large number of molecules in different phases and have been especially useful in the study of protein-membrane interactions [43]. Also, these methods have allowed us to verify experimental data as well as to predict the phenomenon in the absence of other analysis [44,45].

To get insight into the mechanism of the interaction between FABP and membranes, we modeled the process computationally. By using the Finite Difference Poisson Boltzmann Equation (FDPB), we computed the energy involved in the interaction of FABPs with membranes. We show that binding of FABP to membranes involves a significant electrostatic component that discriminates among possible membrane-bound mechanisms and classify a list of FABPs according to the mechanism involved in the interaction. The classification proposed and the results of this model are in agreement with experimental observations for FABP–membrane interaction. Also, our results are in concordance with molecular dynamics simulations that have shown different configurations for the initial interaction between FABPs and membranes [46,47].

2. Materials and methods

2.1. Models and computational procedure

Protein and membrane atomic models were considered as rigid bodies with explicit atomic details, whereas water and ions were modeled together as a continuum structureless medium. In this way, internal degrees of freedom (i.e. flexibility of lateral chains and chemical reactions) were not taken into account. FABP atomic coordinates were obtained in two different ways: those whose tertiary structures were already known, were obtained from RCSB Protein Data Bank [48] (PDB ID: 1BWY, 1FDQ, 1G5W, 1IFB, 1P6P, 1TVQ, 1T4W, 2JU3, 2Q9S, 3FR4, 3IFB). For those with unreported tertiary structured, homology models of the protein based on the template structures were developed (three letter codes in Table 1). Sequence identity between target and structural templates was calculated by retrieving FABP sequences from Uniprot [49] database with search [50] and then aligned using PROMALS [51]. With the multiple sequence alignment a Hidden Markov profile (HMM) of FABPs was then defined. The latter was then funneled through the HHsearch [52] program to identify the most plausible homologous structural templates. HHsearch is one of the best ones as evaluated from CASP7 experiment [53]. The multiple sequence alignment obtained in this way was used as the reference for the structural prediction of FABP by homology modeling. The sequence alignment between our target proteins and the structural templates were extracted from the multiple sequence alignment considering the entire family. We then constructed 15 different conformations of FABPs based on each of the eight structural templates using Modeller9v3 [54]. These were obtained with randomized initial structures and subsequent optimization by conjugate gradients and simulated annealing. All the three dimensional models of FABPs obtained in this way do not deviate from currently available experimental geometries.

Table 1
FABPs of different species and tissues classified according their suggested "collisional" or "diffusional" mechanism of FA transfer to artificial membranes. The structures were obtained from PDB except for those with three letter code, which were modeled according to Materials and methods.

Species	Tissues				
	Collisional				Diffusional
	Intestine (IFABP)	Brain (BFABP)	Heart (HFABP)	Adipocyte (AFABP)	Liver (LFABP)
Human	1KZW	–	1G5W	1JJX	2F73 2PY1
Rat	1IFB 1IFC	MBR	MHR	MAR	2JU3 2JU7
Mouse	MIM	MBM	MHM		MLM
Bovine	MIB	MBB	1BWY	MAB	MLB
Chicken	MIC	MBC	MHC	MAC	1TVQ
Toad	–	–	–	–	1P6P

Atomic coordinates for the membrane were snapshots generated computationally and equilibrated by molecular dynamics procedures.

As a single component of the neutral membrane, we used 1-palmitoyl-2-oleoyl-phophatidylcholine (POPC) and anionic forms of membranes were utilized with a mix of (POPC) and 1-stearoyl-2-oleoyl-phosphatidylserine (SOPS) in different percentages.

For the membrane building five different systems were constructed with different lipid content: (i) 100% POPC–0% SOPS, (ii) 75% POPC–25% SOPS, (iii) 50% POPC–50% SOPS, (iv) 25% POPC–75% SOPS and (v) 0% POPC–100% SOPS. For all the cases, the same protocol was used, the only different was the content of each lipid: a) Coarse grained (CG) bilayer assembly: in order to create an unbiased bilayer with a random distribution of the lipids, a CG representation of the molecules was used. To do this, the CG lipids and CG water molecules were randomly inserted into the simulation box, depending on the system a different percentage of the POPC or SOPS lipids was used but a total number of 100 lipids was used in all the cases. For all the systems, around 1500 CG water molecules were used. In the systems with SOPS, the total charge was neutralized by the addition of CG Na counter ions. Finally, a molecular dynamics simulation of 100 ns was then performed for each system in order to spontaneously self-assemble the bilayer. b) Final CG bilayer construction: Once the bilayer was assembled, the system was replicated producing a bilayer of 200 lipids, this system was also replicated again and rotated around the Y axis in order to obtain a system of 400 CG lipids with a symmetric composition of the lipids on each monolayer and around 6000 CG water molecules. c) CG bilayer equilibration: A coarse grained molecular dynamics simulation of the system with 400 lipids and symmetric composition was performed for 1.5 ms. This was done in order to ensure the correct equilibration of the coarse grained bilayer. d) Atomistic bilayer construction: Then, the atomistic representation of the bilayer from the coarse-grained ones (reverse transformation) were obtained and minimized using a modified version of Gromacs [55]. In order to check whether the transformation to the new atomistic representation did not incorporate some artifacts, a short MD simulation was performed (only 1 ns). The composition of the final systems was 400 lipids and around 24,000 water molecules (since each CG water molecule is equivalent to 4 atomistic water molecules).

The simulation details for the coarse grained and atomistic dynamics were the following: the temperature of 300 K and pressure of 1 bar were controlled using a Berendsen [56] thermostat and semisotropic barostat, both with a coupling parameter of 3 ps for the CG simulations and 1 ps for the atomistic simulations. Compressibility in all directions was set to 6×10^{-5} bar^{-1} for both types of simulations (corresponding to the compressibility of CG water [57]). A time step of 30 fs was used for the coarse grained simulations and 2 fs for the atomistic simulations. The time scale in the CG simulations was matched to the diffusion coefficient of water by multiplying the time in simulation with a factor of 4. The Martini force field [58] was used for the coarse-grained simulations and the Berger force field for the united atom simulations [59]. A modified version of the gromacs package was used for the reverse transformation protocol. The rest of the simulations were performed using the Gromacs package version 4.5.3 [60].

PQR files (in which atom charges and radii replace the occupancies and B-factors of PDB files) were generated by the PDB2PQR server [61] with the PARSE set of charges [62].

The system composed of FABP and membrane was mapped onto a three-dimensional lattice, in which the corner of each cubic cell represents a small region of the protein, membrane, or solvent. Given that the Debye Length (λ_D) for this system is = 10 Å, the chosen grid (86×86×160 Å) was 30% larger than the system. The position of the grid was fixed, allowing proper cancelation of self energy electrostatic terms.

The electrostatic potential at boundary was set to the values prescribed by a Debye–Huckel model for a single sphere with radius and charge corresponding to those of the protein.

Equal amount of sodium and chloride ions (opposite and equal charges with a radius of 2 Å) was distributed linearly into the solvent cage up to 150 mM concentration. Accessible surface area and volumes were calculated using the algorithm and parameters given by Lee and Richards [63]. The dielectric constants of lattice points located within and outside the molecular surface of the protein and membrane were set to 2.0 and 78.5 D, respectively. Ions were excluded from a region that extends 2 Å from the van der Waals surfaces of the protein and membrane. The electrostatic potential at each lattice point was calculated by solving the linear Poisson–Boltzmann equation numerically with the APBS program, which implements a PMG algorithm [64–66].

2.2. Electrostatic free-energy difference

The solutions of the Poisson–Boltzmann equation were used to calculate the total electrostatic free energy of the system [67]. The electrostatic free energy of interaction, *dE*, is the difference between the electrostatic free energy when the protein is close to the membrane, and the electrostatic free energy when both protein and membrane are far from each other ($dE = E(prot + mem) - E(prot) - E(mem)$). The rigid bodies are located and oriented in space by coordinates: Euler angles, ϕ, θ, ψ, describe rotations of the protein; *r*, locates the protein with respect to the membrane, and *x*, *y* represent translations in the plane of the membrane (*r* is the minimum distance between protein and membrane, measured from the van der Waals surface). We assume that a minimum in *dE* corresponds to a preferred configuration. Energy contributions other than that calculated by the Poisson–Boltzmann equation were neglected.

2.3. Sampling the electrostatic free energy landscape

To calculate the membrane–protein global energy, we used an own developed software. This program massively generates files in PQR-format (see above) for different positions of the protein–membrane system, and these files serve as input for the APBS program. Automation and processing of data before, between, and after running the programs were carried out with Bash scripting languages.

The program varies distance and Euler angles and so we can tabulate $dE(r,\phi,\theta,\psi)$ function. For the orientation angle increments, we sample the configuration space at intervals of, $\Delta\varphi = \Delta\theta = \Delta\varphi = 45°$ ($0° < \varphi < 360°$), ($0° < \theta < 180°$) ($0° < \psi < 360°$), resulting in 256 different relative positions. For relative distance between FABP and membrane, $\Delta r = 0.2$ Å was elected.

3. Results and discussions

Electrostatic interactions with negatively charged membranes were computed for the protein-membrane systems employing FABPs of different sources. Table 1 lists the structures of FABPs used. The four letter code corresponds to PDB ID, and the three letter code indicates structures not deposited in PDB and modeled by homology according to Materials and methods.

Initial calculations indicate that $dE = dE(r,\phi,\theta,\psi,x,y)$ could be simplified to $dE = dE(r,\phi,\theta,\psi)$, because changes in *x*, *y* have little impact on *dE* (not shown). The large number of configurations sampled, (256 for each calculation) ensures that the calculated minimum is the global minimum.

All FABPs listed in Table 1 were used to calculate the electrostatic free energy of membrane–protein interaction employing POPC:SOPS membranes of different ratios in order to determine the most plausible configuration for the interaction in each case.

As a neutral membrane, we used a membrane with only POPC. Different anionic forms of membranes were obtained mixing POPC and SOPS in the following ratios 1:0, 3:1, 1:1, 1:3 and 0:1. The utilization of high content of SOPS in model membranes seems to acquire more relevance regarding the recent observation of nanoclusters where PS is concentrated in membranes [68].

While the analysis was made for all structures in Table 1; for clarity, Fig. 1 plots the electrostatic free energy versus 256 different configurations of the FABP–membrane complex for representative members of differentiated groups. Fig. 1a corresponds to an experimentally defined collisional FABP (IFABP from rat) and Fig. 1b corresponds to an experimentally defined diffusional FABP (LFABP from rat). In both figures, each curve indicates different membrane POPC:SOPS ratios. Weak interactions are detected between FABPs of either group and zwitterionic membranes, but an increase in the interaction is observed when SOPS is added to the membranes. Several experiments previously performed have also shown FABP's sensitivity to negatively charged vesicles, especially in the case of IFABP [35–37].

Fig. 1c, superpose the curves for IFABP and LFABP vs. membranes with 25% SOPS content, to show more clearly that the minimum in each case is in a different relative protein–membrane positions. The results, obtained for all the structures analyzed, show a clear differentiation between two groups, which is coincident with the classification based on experimental analysis, as indicated in Table 1. The proteins belonging to the collisional group show a more favorable configuration for the interaction of FABP–membrane with the helical region pointing to the membrane (Fig. 2a). The members of the diffusional group do not show a defined minimum in all the cases, but in those cases that this minimum may be defined, the most probable configuration does not involve the helical region despite the interaction could yet be guided by an electrostatic component. (Fig. 2b). In this regard, electrostatic potential contour analysis of several members of the FABP family [69] has shown that the charge polarity for several members is due to a positive potential across the top of the molecule (helix-turn-helix) and a negative potential in the lower half of the molecule. LFABP is the only LBP of those examined, that has positive and negative potentials in the helix-turn-helix top of the molecule. Studies with mutant and chimeric proteins have demonstrated the crucial importance of the

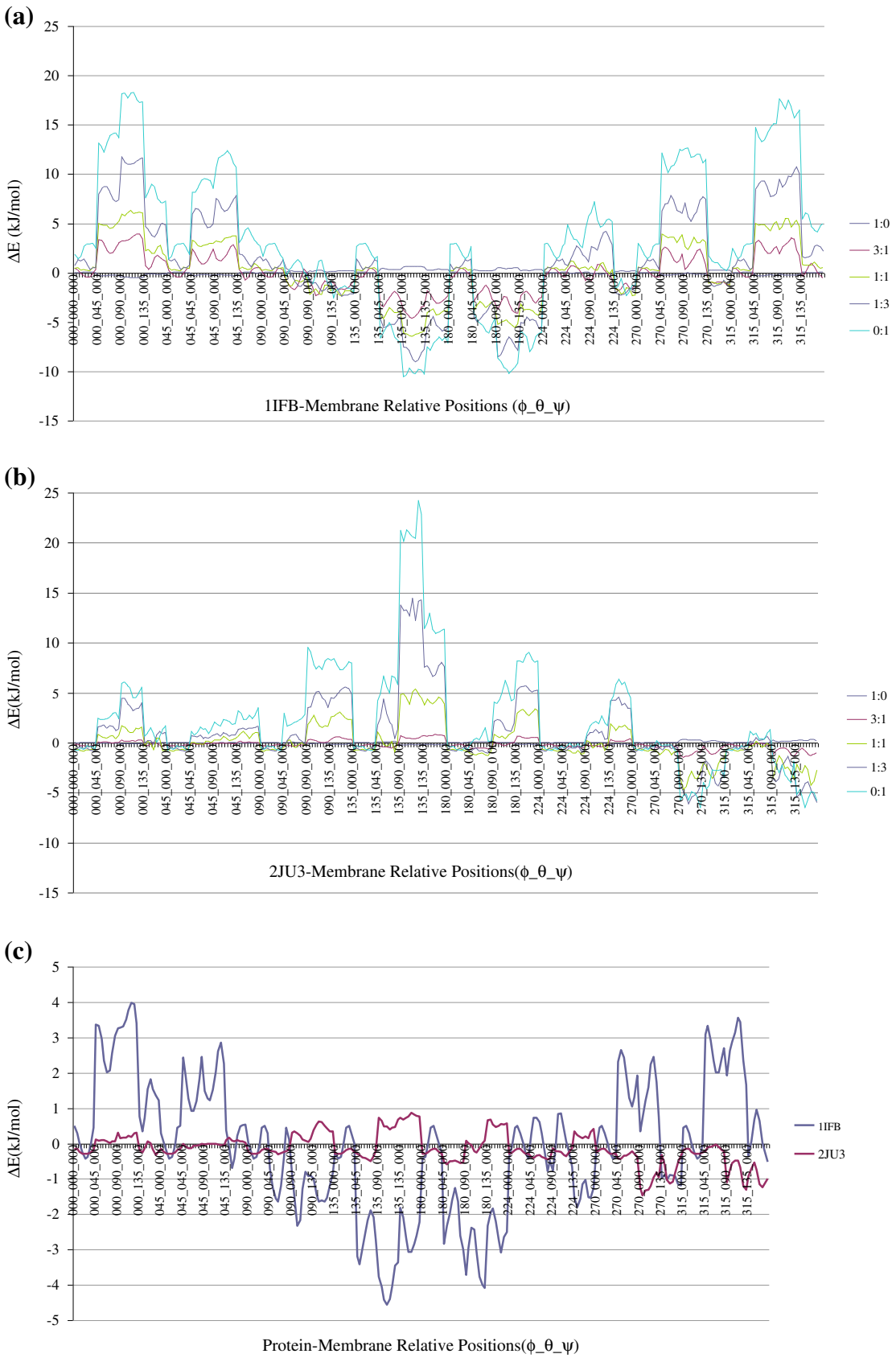

Fig. 1. Electrostatic free energy versus different configurations of FABP–membrane complex for representative members of differentiated groups in Table 1. Tics in x-axis indicate 256 evaluated relative positions in function of Euler angles (φ_θ_ψ). The starting point is a random position, but always the same. For clarity, only φ and θ variations were labeled (View text for values of angles). In Fig. 1a and 1b, curves with different colors indicate different membrane POCP:SOPS ratios (values in inset). (a) Experimentally defined collisional FABP (IFABP from rat), (b) experimentally defined diffusional FABP (LFABP from rat). (c) Overlap of curves extracted of Fig. 1a and 1b respectively for IFABP and LFABP vs. membrane with 25% SOPS content. This clearly shows that the minimum in each case corresponds to different relative protein–membrane positions. These more favored configurations are shown in Fig. 2a and b, respectively.

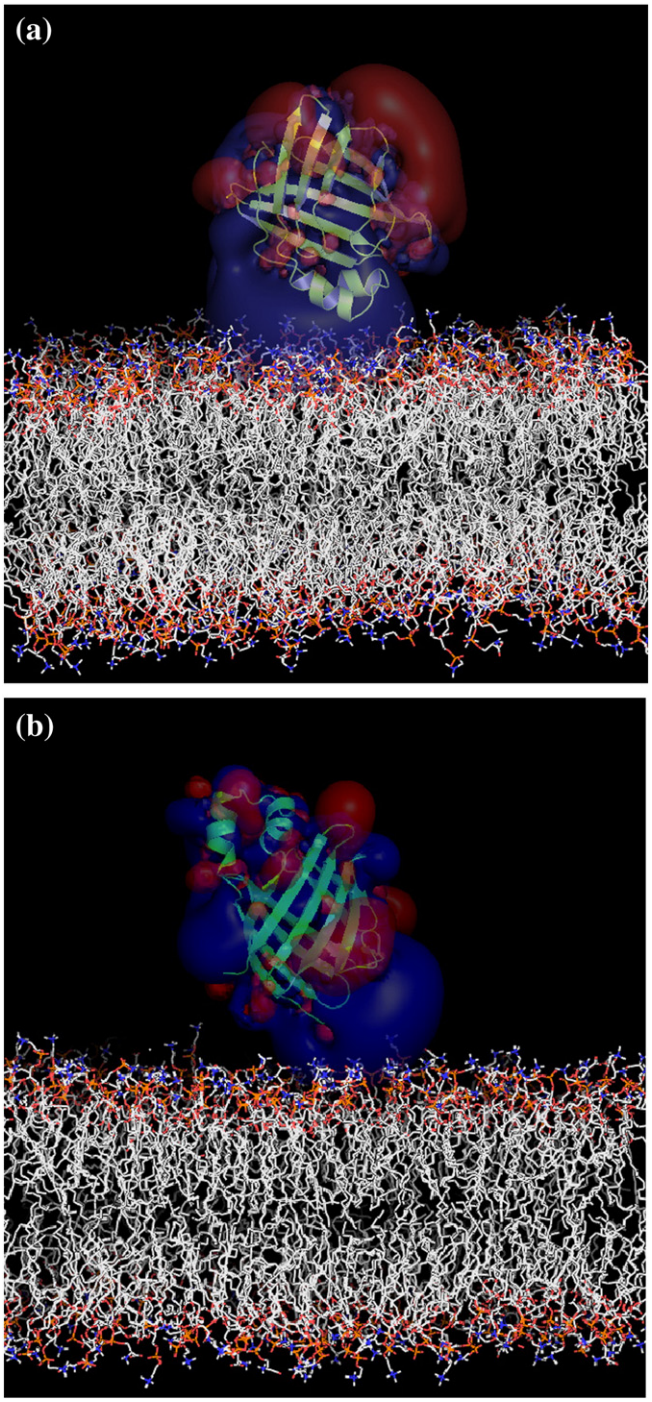

Fig. 2. (a) View of IFABP–membrane complex in the configuration of minimum energy showing the helical region of the protein pointing toward the membrane. (b) View of LFABP–membrane complex also in the configuration of minimum energy. In both graphics the surfaces surrounding the molecules correspond to positive (blue) and negative (red) equipotential energy surfaces due to charge distribution.

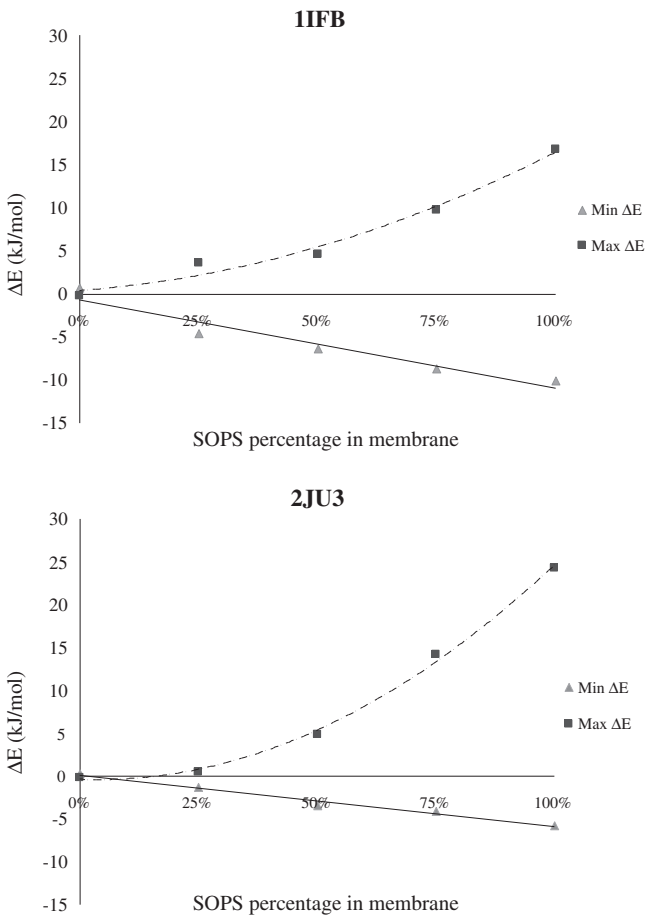

Fig. 3. Electrostatic free energy of IFABP and LFABP vs POPC:SOPS ratio. Values corresponding to most favorable configurations (▲) have soft and lineal decreasing; while less favorable relative positions (■) increase exponentially nominal values of free interaction energy.

alpha-helical region of IFABP in protein–membrane interaction. Our recent experimental work has shown that LFABP also interacts with membranes, although we have not been able to demonstrate yet through experimental work, which are the domain/domains responsible for such interaction [39].

An interesting finding of the results appears viewing Fig. 1a and b. Once the optimal orientation for all cited structures was obtained and the differentiation in two groups was established, we plot the electrostatic free energy of the interaction for one representative molecule of each group, as a function of SOPS content (Fig. 3). When anionic composition of the membrane was changed, energy values corresponding to most favorable configurations have soft and lineal decreasing, while less favorable relative positions increased exponentially nominal values of free interaction energy (Fig. 3). This could be indicating that the increase in anionic phospholipids in the membrane does not produce a much more intensive effect of attraction for favorable configurations, but a major effect of repulsion for not favorable configurations.

Also, the dependence of dE with the distance between van der Waals surfaces for a structure representative of each group and membranes for 25% (SOPS:POPC = 1:3) anionic membranes was analyzed (Fig. 4). The interaction is most favorable at a distance of about (3.5 ± 0.5) Å, but is still significant at a distance of 10 Å corresponding to a characteristic Debye length distance over which the magnitude of electrostatic interactions decrease by approximately $1/e$.

When dependence on ionic strength for LFABP and IFABP was calculated, the behavior in both cases was similar.

Generally, high salt concentrations diminish the effective surface charge of acidic membranes; this charge shielding would consequently be expected to reduce the electrostatic interactions between positively charged residues on the surface and negatively charged headgroups of membrane phospholipids.

For this analysis, the percentage of NaCl was changed and molarity values of 0.001, 0.01, 0.1 and 1.0 M were utilized. Fig. 5 shows how the electrostatic attraction between FABP and a negatively charged membrane is increased as the ionic strength of the solution decreases.

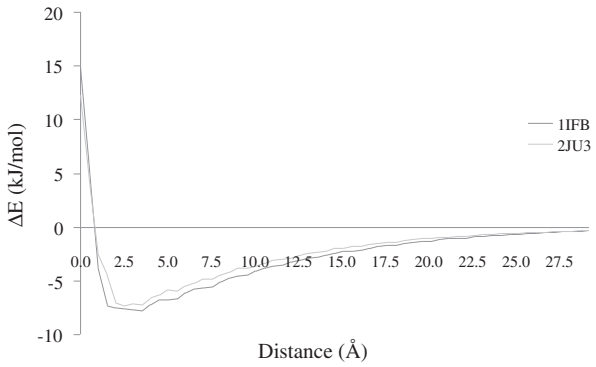

Fig. 4. Plot of electrostatic free energy of IFABP (black) and LFABP (gray) vs protein–membrane distance. Most favorable interaction is for (3.5 ± 0.5) Å between protein–membrane van der Waals surfaces.

These results are consistent with experimental data where the effect of ionic strength for AFABP and acidic membrane was observed [70].

The calculated minimum electrostatic free energy configuration of the system predicted by us, suggests a unique orientation for all the experimentally proposed "collisional" FABPs. The relative position of FABP to the membrane shows the α-helical region involved in the interaction, favoring the strategical position of Lysine charged residues. These results are in complete agreement with experimental data, where, evaluation of the structural elements underlying the mechanism of FA transfer from FABPs has identified the helix-turn-helix domain, and specifically its Lys residues, as the major determinant of the collisional FA transfer mechanism [29]. Moreover, different experimental approaches have shown that the alpha-helical domain is crucial for FABP–membrane interaction [35,39].

On the other hand the configuration for the experimentally proposed "diffusional" FABPs is not well defined, and the minima, if it exists, doesn't show the helical domain directly facing the membrane. However an electrostatic mediated mechanism could be responsible for the interaction. Experimental approaches have indicated that LFABP is able to interact with membranes and that electrostatic interactions seem to play an important role [39]. Nevertheless the domain/domains involved in the interaction are still not known. Other authors, employing tryptophan-containing mutants of LFABP and under conditions of low ionic strength, have suggested the existence of electrostatic interactions which can result in the binding of LFABP to small anionic phospholipid vesicles, through the amino terminus of LFABP [71]. The existence of an amino-terminal exit generated by conformational changes upon ligand binding, has also been suggested. Moreover, in AFABP, an alternative portal located in the N-terminus region has been proposed by other authors employing molecular dynamic simulation [72].

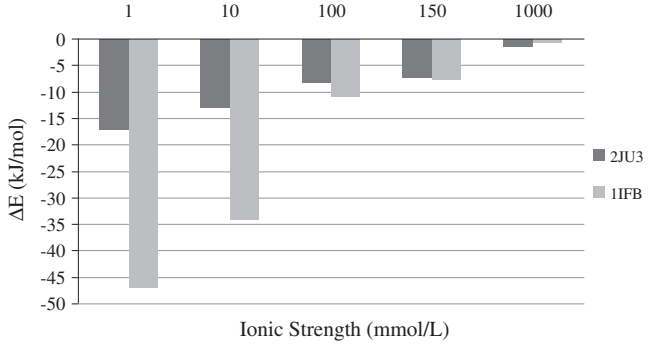

Fig. 5. Bar graphic of the electrostatic free energy of IFABP (black) and LFABP (gray), in their computationally determinate optimal orientations vs ionic strength.

4. Conclusions

The fact that FABPs participate in the intracellular transport of long-chain fatty acids implies that these proteins may be involved not only in the delivery of ligand to acceptor sites, but also in the extraction of fatty acids from donor sites, for instance their removal from the plasma membrane. A relativity fast computational method is used to analyze mechanisms of FABP–membrane interaction of different members of the FABP family of proteins.

Although, the most favored configuration of the system was defined only for electrostatic interactions, our calculations may be capturing essential features of the system despite neglecting the other energy terms. On this basis, it can be hypothesized that: (a) electrostatic free energy is the main driving force for IFABP binding to membranes in a collisional mechanism, with direct interaction between the protein and the membrane via the helical region of the protein. On the other hand, although LFABP–membrane interaction is uncertain, our results shown that the electrostatic term could drive this interaction employing a different mechanism where the helical region is not initially involved. (b) Increasing of anionic composition in membranes doesn't produce a much more intensive effect of attraction for favorable configurations, but a major effect of repulsion between the membrane and not favorable relative positions of the protein. c) Optimal distance between van der Waals surfaces, for FABP-membrane interaction, was approximately 3.5 Å, consistent with previous results in other proteins. Also, electrostatic attraction between FABP and a negatively charged membrane increased as the ionic strength of the solution decreases

These ideas provide, from a computational model, a rational framework where the obtained results allow a starting point for the design of new simulations and/or bench experiments with time and resources economy, aimed to further define more precisely the mechanism of the interaction.

Acknowledgements

We thank Diego Vallejo for his fruitful comments on this manuscript, and Nestor Sanchez Fornillo for his technical assistance. This work has been supported by ANPCyT and Universidad Nacional del Sur (UNS), Bahía Blanca. FZ is a fellow of ANPCyT. FH and BC are members of CONICET.

References

[1] A.H. Talasaz, M. Nemat-Gorgani, Y. Liu, P. Ståhl, R.W. Dutton, M. Ronaghi, R.W. Davis, Prediction of protein orientation upon immobilization on biological and nonbiological surfaces, Proc. Natl. Acad. Sci. USA 103 (40) (2006) 14773–14778.
[2] O. Domènech, L. Redondo, M.T. Montero, J. Hernandez-Borrell, Specific adsorption of cytochrome C on cardiolipin-glycerophospholipid monolayers and bilayers, Langmuir 23 (10) (2007) 5651–5656.
[3] M.R. Lourenzoni, A.M. Namba, L. Caseli, L. Degrève, M.E. Zaniquelli, Study of the interaction of human defensins with cell membrane models: relationships between structure and biological activity, J. Phys. Chem. B 111 (38) (2007) 11318–11329.
[4] F. Bringezu, S. Wen, S. Dante, T. Hauss, M. Majerowicz, A. Waring, The insertion of the antimicrobial peptide dicynthaurin monomer in model membranes: thermodynamics and structural characterization, Biochemistry 46 (19) (2007) 5678–5686.
[5] S.K. Kandasamy, R.G. Larson, Effect of salt on the interactions of antimicrobial peptides with zwitterionic lipid bilayers, Biochim. Biophys. Acta, Biomembr. 1758 (2006) 1274–1284.
[6] J.C. Clayton, E. Hughes, D.A. Middleton, The cytoplasmic domains of phospholamban and phospholemman associate with phospholipid membrane surfaces, Biochemistry 44 (2005) 17016–17026.
[7] R.F. Epand, J.C. Martinou, M. Fornallaz-Mulhauser, D.W. Hughes, R.M. Epand, The apoptotic protein tBid promotes leakage by altering membrane curvature, J. Biol. Chem. 277 (2002) 32632–32639 Epub 2002 Jun 24.
[8] O. Terrones, B. Antonsson, H. Yamaguchi, H.G. Wang, J. Liu, R.M. Lee, A. Herrmann, G. Basanez, Lipidic pore formation by the concerted action of proapoptotic BAX and tBID, J. Biol. Chem. 279 (2004) 30081–30091 Epub 2004 May 11.
[9] L. Vaccaro, K.J. Cross, J. Kleinjung, S.K. Straus, D.J. Thomas, S.A. Wharton, J.J. Skehel, F. Fraternali, Plasticity of influenza haemagglutinin fusion peptides and their interaction with lipid bilayers, Biophys. J. 88 (2005) 25–36.

[10] J. Torres, J. Wang, K. Parthasarathy, D.X. Liu, The transmembrane oligomers of coronavirus protein E, Biophys. J. 88 (2005) 1283–1290.
[11] T. Hughes, B. Strongin, F.P. Gao, V. Vijayvergiya, D.D. Busath, R.C. Davis, AFM visualization of mobile influenza A M2 molecules in planar bilayers, Biophys. J. 87 (2004) 311–322.
[12] T.A. Harroun, K. Balali-Mood, I. Gourlay, J.P. Bradshaw, The fusion peptide of simian immunodeficiency virus and the phase behaviour of N-methylated dioleoylphosphatidylethanolamine, Biochim. Biophys. Acta 1617 (2003) 62–68.
[13] P. Provitera, F. Bouamr, D. Murray, C. Carter, S. Scarlata, Binding of equine infectious anemia virus matrix protein to membrane bilayers involves multiple interactions, J. Mol. Biol. 296 (2000) 887–898.
[14] X. Han, L.K. Tamm, pH-dependent self-association of influenza hemagglutinin fusion peptides in lipid bilayers, J. Mol. Biol. 304 (2000) 953–965.
[15] J.K. Ghosh, S.G. Peisajovich, Y. Shai, Sendai virus internal fusion peptide: structural and functional characterization and a plausible mode of viral entry inhibition, Biochemistry 39 (2000) 11581–11592.
[16] C. Arnulphi, S.A. Sanchez, M.A. Tricerri, E. Gratton, A. Jonas, Interaction of human apolipoprotein A-I with model membranes exhibiting lipid domains, Biophys. J. 89 (2005) 285–295.
[17] K.H. Kim, T. Ahn, C.H. Yun, Membrane properties induced by anionic phospholipids and phosphatidylethanolamine are critical for the membrane binding and catalytic activity of human cytochrome P450 3A4, Biochemistry 42 (2003) 15377–15387.
[18] D. Sahoo, P.M. Weers, R.O. Ryan, V. Narayanaswami, Lipid-triggered conform ational switch of apolipophorin III helix bundle to an extended helix organization, J. Mol. Biol. 321 (2002) 201–214.
[19] B.M. Tandia, C. Lonez, M. Vandenbranden, J.M. Ruysschaert, A. Elouahabi, Lipid mixing between lipoplexes and plasma lipoproteins is a major barrier for intravenous transfection mediated by cationic lipids, J. Biol. Chem. 280 (2005) 12255–12261.
[20] G.J. van der Vusse, M. van Bilsen, J.F. Glatz, D.M. Hasselbaink, J.J. Luiken, Critical steps in cellular fatty acid uptake and utilization, Mol. Cell. Biochem. 239 (2002) 9–15.
[21] A.W. Zimmerman, J.H. Veerkamp, New insights into the structure and function of fatty acid-binding proteins, Cell. Mol. Life Sci. 59 (2002) 1096–1116.
[22] J. Storch, A.E. Thumser, The fatty acid transport function of fatty acid-binding proteins, Biochim. Biophys. Acta 1486 (2000) 28–44.
[23] B.B. Kragelund, J. Knudsen, F.M. Poulsen, Acyl-coenzyme A binding protein (ACBP), Biochim. Biophys. Acta 1441 (1999) 150–161.
[24] U. Seedorf, P. Ellinghaus, J. Roch Nofer, Sterol carrier protein 2, Biochim. Biophys. Acta. 1486 (2000) 45–54.
[25] H. Huang, J.M. Ball, J.T. Billheimer, F. Schroeder, The sterol carrier protein-2 amino terminus: a membrane interaction domain, Biochemistry 38 (40) (1999) 13231–13243.
[26] K.J. Davies, R.M. Hagan, D.C. Wilton, Effect of charge reversal mutations on the ligand- and membrane-binding properties of liver fatty acid-binding protein, J. Biol. Chem. 277 (50) (2002) 48395–48402.
[27] H. Chao, G.G. Martin, W.K. Russell, S.D. Waghela, D.H. Russell, F. Schroeder, A.B. Kier, Membrane charge and curvature determine interaction with Acyl-CoA binding protein (ACBP) and fatty acyl-CoA targeting, Biochemistry 41 (2002) 10540–10553.
[28] N.M. Bass, Function and regulation of hepatic and intestinal fatty acid binding proteins, Chem. Phys. Lipids 38 (1985) 95–114.
[29] J. Storch, B. Corsico, The emerging functions and mechanisms of mammalian fatty acid-binding proteins, Annu. Rev. Nutr. 28 (2008) 73–95.
[30] J. Storch, L. McDermott, Structural and functional analysis of fatty acid binding proteins, J. Lipid Res. 50 (2009) S126–S131 (Suppl.).
[31] H. Wang, Y. He, C.D. Kroenke, S. Kodukula, J. Storch, A.G. Palmer, RE Stark Titration and exchange studies of liver fatty acid-binding protein with ^{13}C-labeled long-chain fatty acids, Biochemistry 41 (17) (2002) 5453–5461.
[32] F.C. Zhang, L.J. Lucke Baier, J.C. Sacchettini, J.A. Hamilton, Solution structure of human intestinal fatty acid binding protein with a naturally-occurring single amino acid substitution (A54T) that is associated with altered lipid metabolism, Biochemistry 42 (2003) 7339–7347.
[33] M.M. Vork, J.F.C. Glatz, G.J. van der Vusse, Modeling intracellular fatty acid transport—possible mechanistic role of cytoplasmic fatty acid-binding protein. Prostaglandins Leukotrienes Essent, Fatty Acids 57 (1997) 11–16.
[34] K.T. Hsu, J. Storch, Fatty acid transfer from liver and intestinal fatty acid-binding proteins to membranes occurs by different mechanisms, J. Biol. Chem. 271 (1996) 13317–13323.
[35] B. Corsico, D.P. Cistola, C. Frieden, J. Storch, The helical domain of intestinal fatty acid binding protein is critical for collisional transfer of fatty acids to phospholipid membranes, Proc. Natl. Acad. Sci. USA 95 (1998) 12174–12178.
[36] B. Corsico, G.R. Franchini, K.T. Hsu, J.J. Storch, Fatty acid transfer from intestinal fatty acid binding protein to membranes: electrostatic and hydrophobic interactions, Lipid Res. 46 (8) (Aug 2005) 1765–1772.
[37] L.J. Falomir-Lockhart, L. Laborde, P.C. Kahn, J. Storch, B. Córsico, Protein-membrane interaction and fatty acid transfer from intestinal fatty acid-binding protein to membranes. Support for a multistep process, J. Biol. Chem. 281 (20) (2006) 13979.
[38] G.R. Franchini, J. Storch, B. Corsico, The integrity of the alpha-helical domain of intestinal fatty acid binding protein is essential for the collision-mediated transfer of fatty acids to phospholipid membranes, Biochim. Biophys. Acta 81 (4) (2008) 192–199.
[39] L.J. Falomir -Lockhart, G.R. Franchini, M. Guerbi, J. Storch, B. Córsico, Interaction of enterocyte FABPs with phospholipid membranes: clues for specific physiological roles, Biochim. Biophys. Acta 1811 (7-8) (2011) 452–459.
[40] B.H. Honig, A. Nicholls, Classical electrostatics in biology and chemistry, Science 268 (1995) 1144–1149.
[41] N. Ben-Tal, B. Honig, R.M. Peitzsch, G. Denisov, S. McLaughlin, Binding of small basic peptides to membranes containing acidic lipids: theoretical models and experimental results, Biophys. J. 71 (1996) 561–575.
[42] N.A. Baker, D. Sept, S. Joseph, M.J. Holst, J.A. McCammon, Electrostatics of nanosystems: application to microtubules and the ribosome, Proc. Natl. Acad. Sci. USA 98 (2001) 10037–10041.
[43] A. Mulgrew-Nesbitt, K. Diraviyam, J. Wang, S. Singh, P. Murray, Z. Li, L. Rogers, N. Mirkovic, D. Murray, The role of electrostatics in protein–membrane interactions, review, Biochim. Biophys. Acta 1761 (2006) 812–826.
[44] M.D. Costabel, D. Vallejo, J.R. Grigera, Electrostatic recognition between enzyme and inhibitor: interaction between papain and leupeptin, Arch. Biochem. Biophys. 394 (2) (2001) 161–166.
[45] D. Vallejo, F. Zamarreño, D.M.A. Guérin, J.R. Grigera, M.D. Costabel, Prediction of the most favored configuration in the ACBP-Membrane interaction based on electrostatic calculations, Biochim. Biophys. Acta, Biomembr. 1788 (2009) 696–700.
[46] M.A. Villarreal, M. Perduca, H.L. Monaco, G.G. Montich, Binding and interactions of L-BABP to lipid membranes studied by molecular dynamic simulations, Biochim. Biophys. Acta 1778 (2008) 1390–1397.
[47] M. Mihajlovic, T. Lazaridis, Modeling fatty acid delivery from intestinal fatty acid binding protein to a membrane, Protein Sci. 16 (2007) 2042–2055.
[48] H.M. Berman, J. Westbrook, Z. Feng, G. Gilliland, T.N. Bhat, H. Weissig, I.N. Shindyalov, P.E. Bourne, The Protein Data Bank, Nucleic Acids Res. 28 (2000) 235–242.
[49] http://www.uniprot.org.
[50] Pearson, Lipman, Proc. Natl. Acad. Sci. 85 (1988) 2444–2448.
[51] PROMALS: towards accurate multiple sequence alignments of distantly related proteins. Jimin Pei and Nick V. Grishin, Bioinformatics 23 (7) (2007) 802–808, doi:10.1093/bioinformatics/btm017.
[52] J. Söding, Protein homology detection by HMM–HMM comparison, Bioinformatics 21 (7) (2005) 951–960.
[53] J. Moult, J.T. Pedersen, R. Judson, K. Fidelis, A large-scale experiment to assess protein structure prediction methods, Proteins 23 (3) (1995) ii–iv.
[54] N. Eswar, M.A. Marti-Renom, B. Webb, M.S. Madhusudhan, D. Eramian, M. Shen, U. Pieper, A. Sali, Comparative protein structure modeling with MODELLER, Current Protocols in Bioinformatics, Supplement, 15, John Wiley & Sons, Inc., 2006, pp. 5.6.1–5.6.30.
[55] A.J. Rzepiela, L.V. Schafer, N. Goga, H.J. Risselada, A.H. de Vries, S.J. Marrink, Reconstruction of atomistic details from coarse-grained structures, J. Comput. Chem. 31 (2010) 1333–1343.
[56] H.J.C. Berendsen, J.P.M. Postma, W.F. van Gunsteren, A. DiNola, J.R. Haak, Molecular dynamics with coupling to an external bath, J. Chem. Phys. 81 (1984) 3684–3690.
[57] S.J. Marrink, A.H. de Vries, A.E. Mark, Coarse grained model for semi-quantitative lipid simulations, J. Phys. Chem. B 108 (2004) 750–760.
[58] S.J. Marrink, H.J. Risselada, S. Yefimov, D.P. Tieleman, A.H. de Vries, The MARTINI force field: coarse grained model for biomolecular simulations, J. Phys. Chem. B 111 (2007) 7812–7824.
[59] O. Berger, O. Edholm, F. Jahnig, Molecular dynamics simulations of a fluid bilayer of dipalmitoylphosphatidylcholine at full hydration, constant pressure, and constant temperature, Biophys. J. 72 (1997) 2002–2013.
[60] D. Van Der Spoel, E. Lindahl, B. Hess, G. Groenhof, A.E. Mark, H.J. Berendsen, GROMACS: fast, flexible, and free, J. Comput. Chem. 26 (2005) 1701–1718.
[61] T.J. Dolinsky, J.E. Nielsen, J.A. McCammon, N.A. Baker, PDB2PQR: an automated pipeline for the setup, execution, and analysis of Poisson–Boltzmann electrostatics calculations, Nucleic Acids Res. 32 (2004) W665–W667.
[62] D. Sitkoff, K.A. Sharp, B. Honig, Accurate calculation of hydration free energies using macroscopic solvent models, J. Phys. Chem. 98 (1994) 1978–1988.
[63] B. Lee, F.M. Richards, The interpretation of protein structures: estimation of static accessibility, J. Mol. Biol. 55 (3) (1971) 379–400.
[64] N.A. Baker, D. Sept, S. Joseph, M.J. Holst, J.A. McCammon, Electrostatics of nanosystems: application to microtubules and the ribosome, Proc. Natl. Acad. Sci. U. S. A. 98 (2001) 10037–10041.
[65] M. Holst, F. Saied, Multigrid solution of the Poisson–Boltzmann equation, J. Comput. Chem. 14 (1993) 105–113.
[66] M. Holst, F. Saied, Numerical solution of the nonlinear Poisson–Boltzmann equation: developing more robust and efficient methods, J. Comput. Chem. 16 (1995) 337–364.
[67] M.K. Gilson, B. Honig, Calculation of the total electrostatic energy of a macromolecular system: solvation energies, binding energies, and conformational analysis, Prot. Struct. Funct. Gen. 4 (1988) 7–18.
[68] G.D. Fairn, N.L. Schieber, N. Ariotti, S. Murphy, L. Kuerschner, R.I. Webb, S. Grinstein, R.G. Parton, High-resolution mapping reveals topologically distinct cellular pools of phosphatidylserine, J. Cell Biol. 194 (2) (2011) 257–275.
[69] V.J. LiCata, D.A. Bernlohr, Surface properties of adipocyte lipid-binding protein: response to lipid binding, and comparison with homologous proteins, Prot. Struct. Funct. Gen. 33 (1998) 577–589.
[70] E.R. Smith, J. Storch, The adipocyte fatty acid-binding protein binds to membranes by electrostatic interactions, J. Biol. Chem. 274 (50) (1999) 35325–35330.
[71] J.K. Davies, A.E. Thumser, D.C. Wilton, Binding of recombinant rat liver fatty acid-binding protein to small anionic phospholipid vesicles results in ligand release: a model for interfacial binding and fatty acid targeting, Biochemistry 38 (51) (1999) 16932–16940.
[72] R. Friedman, E. Nachliel, M. Gutman, Molecular dynamics simulations of the adipocyte lipid binding protein reveal a novel entry site for the ligand, Biochemistry 44 (11) (2005) 4275–4283.